Computation of the water density distribution at the ice-water interface using the potentials-of-mean-force expansion

Gerhard Hummer[1] and Dikeos Mario Soumpasis[2]
[1] *Theoretical Biology and Biophysics Group T-10, Los Alamos National Laboratory, Los Alamos, New Mexico 87545*
[2] *Molecular Biology Department, Max Planck Institute for Biophysical Chemistry, P.O. Box 2841, D-37018 Göttingen, Germany*
(Received 11 August 1993)

The water density distribution at an ice-I*h*–water interface is computed by means of the expansion of the n-particle potentials of mean force (PMF) in terms of lower-order PMF's truncated at the triplet level. Pair and triplet correlations for the simple point-charge water model are computed via Monte Carlo (MC) simulations. The distributions obtained are in very good agreement with extensive MC simulations of the interface. The PMF-expansion technique is orders of magnitude faster than the simulations and provides a powerful tool for the study of complex interfacial phenomena involving aqueous phases.

PACS number(s): 68.45.−v, 61.20.Gy, 61.25.Em, 82.65.Dp

I. INTRODUCTION

The physical properties of solid-liquid interfaces are of great theoretical and practical interest. Many important processes such as melting, nucleation, crystal growth, chemical reactions, and catalysis take place at interfaces involving aqueous phases. In addition, phenomena at biomolecule-water interfaces play a central role in biological systems. However, in the case of nonsimple liquids, the theoretical description using integral equations and related techniques is seriously hampered owing to the molecular structure of the particles. Unfortunately, computer simulations are also rather limited due to the complexity of most systems of practical interest requiring CPU times much too long to be useful in large-scale investigations of important processes.

An important example is the ice-water interface where, due to the complexity of water as a liquid, even the study of the bulk water phase is a nontrivial task. Recently, a density-functional theory was devised to study the freezing of water using an interaction-site description of the molecule [1]. Also, the density-functional method has been used to study liquids with multipolar interactions [2]. Systems comprising ice and water were analyzed in a series of computer simulation studies using clusters [3], periodic boundary conditions in all directions [4–6], and a slab geometry [7].

Here we apply a relatively simple, efficient, and extremely fast method to calculate the density profile at the ice-water interface. Because of its generality, the method can easily be extended to more complex cases. The approach is based on the expansion of the n-particle potentials of mean force (PMF) in terms of lower-order PMF's [8], truncated at the three-atom correlation level. The conditional density at the ice surface is expressed in terms of atom correlation functions up to triplet level of bulk water. The water pair and triplet correlations are calculated by a Monte Carlo (MC) simulation of bulk water, using a model with molecular details. The quantitative validity of our approach is tested by comparing the water density profiles obtained to those obtained via extensive computer simulation for the same model ice-water interface. A much simpler version of the formalism employing the restricted primitive model of electrolytes and truncating the ionic correlations at the pair level was used by our group to estimate ionic densities around various DNA conformations [9,10].

II. POTENTIALS OF MEAN FORCE EXPANSION

In a simple monoatomic liquid, with n particles fixed at positions $\mathbf{r}_1,\ldots,\mathbf{r}_n$, the effective one-particle density $\rho^{(n,1)}$ at a point $\mathbf{r}$ is given by

$$\rho^{(n,1)}(\mathbf{r}|\mathbf{r}_1,\ldots,\mathbf{r}_n)=\rho\,\frac{g^{(n+1)}(\mathbf{r},\mathbf{r}_1,\ldots,\mathbf{r}_n)}{g^{(n)}(\mathbf{r}_1,\ldots,\mathbf{r}_n)}\ , \tag{1}$$

where $g^{(n)}$ is the n-particle correlation function and ρ is the bulk density. The expansion of the n-particle PMF's defined by

$$W^{(n)}(\mathbf{r}_1,\ldots,\mathbf{r}_n)=-k_{\mathrm{B}}T\ln g^{(n)}(\mathbf{r}_1,\ldots,\mathbf{r}_n) \tag{2}$$

in terms of lower order PMF's yields

$$W^{(n)}(\mathbf{r}_1,\ldots,\mathbf{r}_n)=\sum_{\substack{i,j\\ i>j}} W^{(2)}(\mathbf{r}_i,\mathbf{r}_j) + \sum_{\substack{i,j,\mathrm{h}\\ i>j>k}}\left[W^{(3)}(\mathbf{r}_i,\mathbf{r}_j,\mathbf{r}_k)-W^{(2)}(\mathbf{r}_i,\mathbf{r}_j)-W^{(2)}(\mathbf{r}_j,\mathbf{r}_k)-W^{(2)}(\mathbf{r}_k,\mathbf{r}_i)\right]+\cdots\ . \tag{3}$$

Combining Eqs. (1) and (2), and retaining terms up to the triplet level in the PMF expansion Eq. (3) we obtain an expression for the conditional density in terms of two- and three-particle correlation functions,

$$\rho^{(n,1)}(\mathbf{r}|\mathbf{r}_1,\ldots,\mathbf{r}_n) \approx \rho \prod_{i=1}^{n} g^{(2)}(\mathbf{r},\mathbf{r}_i) \prod_{j=1}^{n-1} \prod_{k=j+1}^{n} \frac{g^{(3)}(\mathbf{r},\mathbf{r}_j,\mathbf{r}_k)}{g^{(2)}(\mathbf{r},\mathbf{r}_j) g^{(2)}(\mathbf{r}_j,\mathbf{r}_k) g^{(2)}(\mathbf{r}_k,\mathbf{r})} \; . \tag{4}$$

Truncation of Eq. (3) at the pair level corresponds to the Kirkwood superposition approximation (KSA) [11] for the triplet correlation function,

$$g^{(3)}(\mathbf{r}_1,\mathbf{r}_2,\mathbf{r}_3) = g^{(2)}(\mathbf{r}_1,\mathbf{r}_2) g^{(2)}(\mathbf{r}_2,\mathbf{r}_3) g^{(2)}(\mathbf{r}_3,\mathbf{r}_1) \; ; \tag{5}$$

retaining the triplet contribution is equivalent to the Fisher-Kopeliovich superposition approximation [12] for the four-particle correlation function,

$$g^{(4)}(\mathbf{r}_1,\mathbf{r}_2,\mathbf{r}_3,\mathbf{r}_4) = \frac{\prod\limits_{\substack{i,j,k \\ i<j<k}} g^{(3)}(\mathbf{r}_i,\mathbf{r}_j,\mathbf{r}_k)}{\prod\limits_{\substack{i,j \\ i<j}} g^{(2)}(\mathbf{r}_i,\mathbf{r}_j)} \; . \tag{6}$$

It is also possible to calculate particle-particle correlations in inhomogeneous systems using the PMF expansion formalism. (For example, pair correlations are needed to calculate thermodynamic quantities such as the surface tension [13].) This is accomplished by factorizing the two-particle density in terms of conditional one-particle densities that can be calculated using Eq. (4),

$$\rho^{(n,2)}(\mathbf{r},\mathbf{s}|\mathbf{r}_1,\ldots,\mathbf{r}_n) = \rho^{(n+1,1)}(\mathbf{r}|\mathbf{s},\mathbf{r}_1,\ldots,\mathbf{r}_n) \times \rho^{(n,1)}(\mathbf{s}|\mathbf{r}_1,\ldots,\mathbf{r}_n) \; . \tag{7}$$

To model an ice-water interface, we fix n water oxygens at ideal ice Ih lattice positions $\mathbf{r}_1,\ldots,\mathbf{r}_n$, but we do not specify the molecular orientations of the water molecules. The n water molecules in the ice configuration are then embedded in liquid water. An increase of disorder in the ice layers near the interface is restricted to the reorientation of water hydrogens, giving some flexibility in the formation of the hydrogen bond network. This somewhat simplified picture of the interface with perfectly ordered oxygens allows a simpler theoretical treatment. Nevertheless, it is realistic enough to describe relevant properties of the real ice-water interface. It should be stressed that even the quite flexible computer simulation methodology faces serious difficulties in the case of inhomogeneous interfacial systems with coexisting phases, one of which is the problem of keeping two phases stable under periodic boundary conditions and for a comparably small number of particles. Moreover, much of the theoretical analysis of interfacial systems at an atomic level has been limited to strongly simplified cases such as hard walls modeling the solid phase.

A possible way to relax the assumption of fixed positions of the oxygen atoms is to introduce an additional averaging over weighted oxygen positions in the ice phase. For example, the positions of the oxygens can be drawn from Gaussian distributions around the lattice sites with widths corresponding to the experimentally observed thermal fluctuations in bulk ice [14]. However, in order to have well-defined conditions that allow a conclusive comparison with computer simulation data for an equivalent system, we here restrict our analysis to the model of fixed oxygen atoms.

As in the case of simple liquids, the oxygen and hydrogen density distributions can be expressed in terms of oxygen and hydrogen pair and triplet correlation functions. For the oxygen and hydrogen density (X=O,H) we obtain

$$\rho_X^{(n,1)}(\mathbf{r}|\mathbf{r}_1,\ldots,\mathbf{r}_n) \approx \rho_X \prod_{i=1}^{n} g_{X\mathrm{O}}^{(2)}(\mathbf{r},\mathbf{r}_i) \prod_{j=1}^{n-1} \prod_{k=j+1}^{n} \frac{g_{X\mathrm{OO}}^{(3)}(\mathbf{r},\mathbf{r}_j,\mathbf{r}_k)}{g_{X\mathrm{O}}^{(2)}(\mathbf{r},\mathbf{r}_j) g_{\mathrm{OO}}^{(2)}(\mathbf{r}_j,\mathbf{r}_k) g_{\mathrm{O}X}^{(2)}(\mathbf{r}_k,\mathbf{r})} \; . \tag{8}$$

In the case of water, it is essential to include the triplet correlations since the preference for tetrahedral, ice-like water configurations with oxygen distances of about 0.275, 0.275, and 0.45 nm definitely leads to deviations from the simple pair picture suggesting equilateral triangles with distances of 0.275 nm to be prevalent. Using the proposed method, studies of various configurations of fixed water molecules can easily be undertaken. Furthermore, the extension of Eq. (8) to the case with hydrogen atoms kept at particular positions in space is straightforward.

III. COMPUTER SIMULATIONS

In order to obtain pair and triplet correlation functions of liquid water, computer simulations of bulk water have to be performed since experiments give only limited access to these quantities. Especially to compute the triplet correlations, quite extensive calculations are necessary. However, these computations have to be done only once (for given ρ and T), and the data can then be used for different applications.

The first computations of triplet correlations in water [15] were perfomed using the *ab initio* Niesar-Clementi-Corongiu water model [16]. In the present study we use the simpler but also satisfactory simple point-charge (SPC) water model [17]. Interaction site descriptions of water such as the SPC model with partial charges distributed on the molecules are able to reproduce basic properties of liquid water reasonably well. In particular, a complex network of hydrogen bonds characteristic for associated liquids is formed. Samples of model water

molecules also show a dielectric screening behavior corresponding to liquid water, although the actual dielectric constants of different models vary considerably. The SPC model is known to yield good results for many structural, dynamic, and thermodynamic quantities despite its simplicity. It is a rigid water model built of one oxygen and two hydrogen interaction sites with an O–H bond length of 0.1 nm and an ideally tetrahedral H–O–H bond angle (109.47°). Partial charges $q_O = -0.82e$ and $q_H = 0.41e$ are placed on the oxygen and hydrogen sites, respectively. In addition, there is a Lennard-Jones interaction between oxygens. (For a discussion of different water models see, e.g., Ref. [18].)

Configuration space averaging was done using the Metropolis Monte Carlo method [19]. The system consisted of 256 water molecules with a particle density of $\rho = 33.33$ nm^{-3} and a temperature of $T = 298$ K. The simulation box used was a rhombic dodecahedron. The Coulomb interactions were treated with a generalized reaction-field (GRF) scheme briefly described in the following using an atom-atom cutoff of $r_c = 0.9$ nm and a background dielectric constant of $\epsilon_{RF} = 65$, which is the approximate value for bulk SPC water [20,21].

The GRF, like previous attempts to devise effective and accurate modified r-dependent Coulomb interactions for liquid systems under periodic boundary conditions [22–26], tries to mimic the effective screening of the bare Coulomb interaction in polar and ionic systems. This screening results from the preference of oppositely charged particles in the surrounding of ions and charged sites. It is most effective in a system of high charge density. In the GRF scheme, of which a detailed description and analysis will be given elsewhere [27], charges q_i and q_j (Gaussian units) in distance r are subject to a modified Coulomb interaction $u(r) = q_i q_j \phi(r)$,

$$\phi(r) = \frac{1}{r}\left(1 - \frac{r}{r_c}\right)^4 \left(1 + \frac{8r}{5r_c} + \frac{2r^2}{5r_c^2}\right) \Theta(r_c - r) \ , \quad (9)$$

where $\Theta(r)$ is the Heaviside unit step function. $\phi(r)$ is the interaction of two unit charges $+1$ surrounded by background charges -1 and $+1$, respectively, homogeneously distributed in spheres with radius $r_c/2$, when all interactions (charge-charge, charge-background, and background-background) are counted. The total Coulomb energy in a molecular system is

$$U_c = \sum_{\substack{i,j,k \\ i<j}} \sum_{\alpha,\beta} q_{i_\alpha} q_{j_\beta} \phi(r_{i_\alpha j_\beta}) + \frac{1}{2} \sum_i \sum_{\alpha,\beta} q_{i_\alpha} q_{i_\beta} \times \lim_{r \to r_{i_\alpha i_\beta}} \left[\phi(r) - \frac{1}{r}\right] + \frac{2\pi \mathbf{M}^2}{(2\epsilon_{RF} + 1)V} \ , \quad (10)$$

where α and β are charged sites on molecules i and j. $\mathbf{M}$ is the total dipole moment of the system and V its volume. The last term corrects the background dielectric constant from infinity to ϵ_{RF} [28]. The GRF Coulomb interaction $\phi(r)$ is of short range and strongly screened. Both $\phi(r)$ and its derivatives up to third order vanish at $r = r_c$. In addition, $\phi(r)$ and its derivatives are monotone and of alternating sign, exactly like the bare Coulomb interaction $1/r$.

In computer simulations of polar and charged systems, the GRF scheme allows an efficient calculation of the Coulomb energy, since only a short-range r-dependent function has to be evaluated, which can be tabulated. The GRF was successfully applied in the study of electrolytes, where it compared perfectly with Ewald summation at various ionic concentrations. Studies of pure water, one component plasmas, and restricted primitive model electrolytes yielded excellent structural (pair and angular correlations) and thermodynamic results [27]. As will be shown in the following, also in the case of inhomogeneous aqueous systems the GRF gives results in agreement with Ewald summation. Here the GRF was used in order to allow a much less time consuming calculation of the electrostatic interactions than with Ewald summation [29].

The methods used for computing pair and triplet correlations were discussed in Ref. [30]. Bin widths of 0.005 and 0.02 nm, respectively, were used. The correlations were sampled for pair distances up to 1.1 and 0.72 nm, respectively. The initial configuration was a random distribution of randomly oriented water molecules. The system was equilibrated for 50 000 passes (one attempted move per particle). The production run then extended over additional 170 000 MC passes.

To provide reliable density data for the ice-water interface, against which the results of the proposed PMF expansion method could be tested, a series of MC simulations of the interfacial system was performed. This was accomplished by positioning 240 water oxygens at ice Ih lattice sites in a rectangular box. The x and y dimensions of the box were chosen to be consistent with the ice lattice ($L_x = 2.245$ nm and $L_y = 2.333$ nm with an oxygen separation of 0.275 nm). The two basal planes of the ice were oriented normal to the z axis and in contact with liquid water. The z thickness of the ice layer was 1.192 nm. Periodic boundary conditions were applied in all directions.

The z dimension of the box was chosen such that the overall density including the ice water molecules was $\rho = 33.33$ nm^{-3}. For total numbers of particles of $N = 600$ and 1000 this results in $L_z = 3.436$ and 5.726 nm, respectively. Both phases were kept at a temperature of $T = 298$ K. In principle, the study could have been done at any temperature, e.g., the temperature of coexisting phases for the water model employed here (see Ref. [6]).

Four simulations with different characteristics were performed. In three of the simulations, the GRF model used in the water triplet calculations was applied with atom-atom cutoffs of $r_c = 0.9$ and 0.8 nm, respectively. In one of the reaction field runs the number of particles was set to $N = 1000$; in all others 600 particles were used.

Also an Ewald summation technique [31] was used in a simulation employing 600 particles to avoid possible ambiguities arising from the treatment of the Coulomb interaction in the inhomogeneous system. The real space damping factor was set to $\eta = 5.6/L_x$. The k-space cutoff was set to $k^2 \leq 22(2\pi/L_x)^2$, resulting in 2×343 k vectors considered. The r-space cutoff was $r_c = 0.93$ nm

and applied atomwise. In all simulations, the background dielectric constant was set to $\epsilon_{RF} = 65$.

In the case of the $N = 600$ and 1000 simulations with GRF Coulomb interaction and $r_c = 0.9$ nm, the starting configurations were randomly distributed mobile water molecules. All water molecules were randomly oriented. The two other simulations started from the final configuration (after 200 000 passes) of the $N = 600$ GRF simulation with $r_c = 0.9$ nm. Averages were taken every tenth pass after 50 000 passes of equilibration. In Table I the characteristics of the simulations are compiled.

IV. RESULTS AND DISCUSSION

In Fig. 1 the oxygen and hydrogen densities are depicted in units of the bulk density versus the z distance of the closest basal plane of the ice layer. The outmost oxygen atoms of the ice layer are at $z = 0$. The curves obtained from the various MC simulations agree well within the statistical errors, which are of the order of 0.1 at the density peaks, as estimated from block averaging. In particular, the Ewald and GRF simulation results do not differ significantly. In the case of the oxygen density a strong peak at $z = 0.26$ nm is followed by several steps reflecting the formation of water layers. However, only the first peak is at a z value consistent with an ice Ih lattice extending into the liquid. The structure beyond the first peak does not correspond with an ideal ice-lattice behavior, for which the predicted peak positions are indicated as arrows in Fig. 1. The hydrogen density also reflects the formation of a first icelike layer of water molecules with the peaks at $z = 0.17$ and 0.30 nm in good agreement with the ideal lattice positions. Again, the structure beyond the first layer is much less distinct. But interestingly, peaks at $z = 0.55$ and 0.7 nm agree quite well with ideal lattice values.

Figure 1 also shows the results of the PMF expansion using Eq. (8) up to pair and triplet level. In the calculation of the densities, the discrete pair and triplet data for water were interpolated linearly. In order to take density averages at constant values of z, for every value of z, 10 000 points were randomly chosen in a hexagon perpendicular to the z axis with the size corresponding to the ice lattice. The pair-level truncation of the PMF expansion yields only a crude picture due to the highly anisotropic nature of the intermolecular interactions in water. It fails especially in the case of the oxygen density at small z. The first peak shown by the pair expansion is due to the incorrect KSA prediction of equilateral triplets with

TABLE I. Characteristics of the ice-water interface MC simulations. N is the particle number, L_z is the z dimension of the box, r_c is the cutoff length, and Coulomb denotes the treatment of the Coulomb interactions.

N	L_z (nm)	Coulomb	r_c (nm)	Passes
600	3.436	GRF	0.90	150 000
600	3.436	GRF	0.80	50 000
600	3.436	Ewald	0.93	50 000
1000	5.726	GRF	0.90	90 000

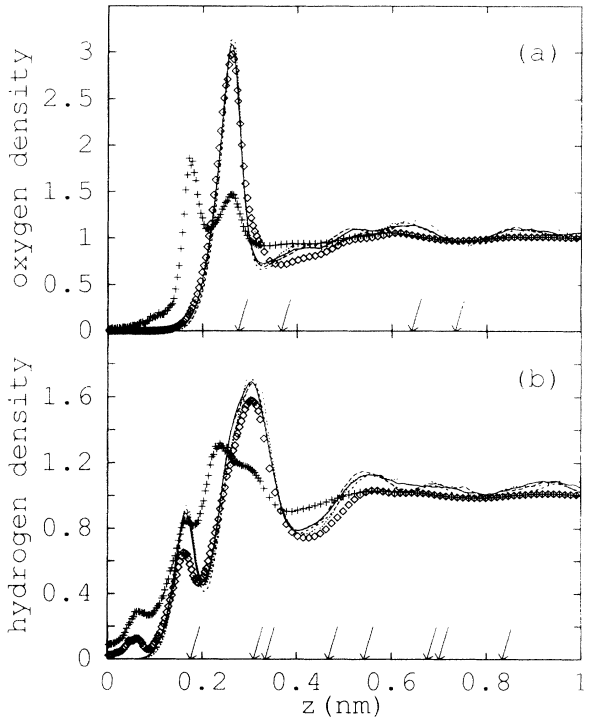

FIG. 1. (a) Water-oxygen and (b) water-hydrogen density at the ice-water interface in units of the corresponding bulk densities. z denotes the z distance from the ice basal plane defined as the outmost layer of oxygen atoms. Arrows indicate the peak positions in the case of an ideal ice Ih lattice. +, PMF expansion including only pairs; ◇, PMF expansion including triplets. MC simulations: (—), GRF, $N = 600$, $r_c = 0.9$ nm; (– –), GRF, $N = 600$, $r_c = 0.8$ nm; (- - -), GRF, $N = 1000$, $r_c = 0.9$ nm; (· · ·), Ewald, $N = 600$.

edges 0.275 nm and does not appear in the simulations. The second peak is at the right position but too small.

However, inclusion of the triplet correlations drastically improves the quality of the results obtained from the PMF expansion. Now both the position and the height of the first peak of the oxygen density are reproduced quantitatively correct. The first minimum is at a somewhat greater z distance, but even for distances between 0.35 and 0.7 nm, the PMF expansion shows qualitatively correct behavior.

The PMF expansion also correctly reproduces the hydrogen density for z values greater than 0.2 nm. The second, strong peak is at the right position and only slightly too low. In addition, both the second minimum and the third maximum are at the correct positions, with the third maximum being somewhat too small. The peak at $z = 0.17$ nm is too small. We ascribe the discrepancies in this region mainly to problems with the discretization of the correlation functions. Within the resolution of the triplet correlations of 0.02 nm, $g^{(2)}_{OH}(r)$ jumps from approximately 0.03 at $r = 0.15$ nm to 1.08 at 0.17 nm. But also sampling problems of the triplet correlation function have to be considered, which are most prominent at small distances. The hydrogen density for $z < d_{OH}$ ($d_{OH} = 0.1$ nm is the O–H bond length of the SPC water model) is also affected by intramolecular correlations.

However, these were not considered in the calculation of the correlation functions. Therefore, the hydrogen density data for $z < 0.1$ nm, describing the distribution of the hydrogens belonging to ice molecules, are not properly represented.

For $z \gtrsim 0.4$ nm the computer simulation data for the oxygen and hydrogen densities exhibit somewhat more structure than the PMF expansion results. The deviations can only partly be ascribed to statistical noise present in the simulation data. The quadruplet and higher-order correlations are expected to add some corrections to the PMF density curves. However, with the available theoretical tools they cannot be calculated nor are they readily accessible from simulations with satisfactory statistical accuracy. A comparably practicable way to obtain the quadruplet correction is to compute the conditional density $\rho^{(3,1)}(\mathbf{r}|\mathbf{r}_1,\mathbf{r}_2,\mathbf{r}_3)$ in a simulation by constraining the pair distances of particles 1, 2, and 3. This has to be done only for the smallest triangles in the basal plane, particularly the one with edges 0.275, 0.275, and 0.449 nm, which is expected to give the largest contribution to the quadruplet correction. $\rho^{(3,1)}$ is related to the four particle correlation function through

$$\rho^{(3,1)}(\mathbf{r}|\mathbf{r}_1,\mathbf{r}_2,\mathbf{r}_3) = \rho\,\frac{g^{(4)}(\mathbf{r},\mathbf{r}_1,\mathbf{r}_2,\mathbf{r}_3)}{g^{(3)}(\mathbf{r}_1,\mathbf{r}_2,\mathbf{r}_3)}\ . \tag{11}$$

Interestingly, independent of system size and Coulomb interaction model (Ewald summation and GRF), the computer simulation curves for the oxygen and hydrogen densities show shallow minima quite far from the actual interface at $z = 0.75$ and 0.8 nm, respectively. The PMF expansion indeed yields corresponding minima at the right positions but less distinct. However, since water triplet data were only available for triangles with all three edges smaller than 0.72 nm, the triplet correction was not applicable in this region.

V. CONCLUDING REMARKS

The study of inhomogeneous aqueous systems is of great importance for the physical description of biological systems and of condensed matter. Using an approach based on an expansion of the n-particle PMF's, we calculated the oxygen and hydrogen density profile at the ice-water interface. Computer simulation data for the same system were quantitatively reproduced. However, the calculation of density distributions using the PMF expansion formula is about 10^2 to 10^4 times faster than computer simulations of the interfacial system, which require typically several days of CPU time. Another advantage of the method is that one can probe the density distribution completely locally, i.e., especially near the region of interest. In addition to its computational efficiency, we also want to emphasize the flexibility of the approach. It is easily adapted to describing physical properties of different inhomogeneous, aqueous systems. Several applications of this method to biological systems will be published in the near future.

ACKNOWLEDGMENTS

We wish to thank our colleagues Angel E. García and Martin Neumann for many valuable discussions and collaborations.

[1] K. Ding, D. Chandler, S. J. Smithline, and A. D. J. Haymet, Phys. Rev. Lett. **59**, 1698 (1987).
[2] See, e.g., P. I. Teixeira and M. M. Telo da Gama, J. Phys. Condens. Matter **3**, 111 (1991).
[3] T. A. Weber and F. H. Stillinger, J. Phys. Chem. **87**, 4277 (1983).
[4] O. A. Karim and A. D. J. Haymet, Chem. Phys. Lett. **138**, 531 (1987).
[5] O. A. Karim and A. D. J. Haymet, J. Chem. Phys. **89**, 6889 (1988).
[6] O. A. Karim, P. A. Kay, and A. D. J. Haymet, J. Chem. Phys. **92**, 4634 (1990).
[7] G.-J. Kroes, Surf. Sci. **275**, 365 (1992).
[8] A. Münster, *Statistical Thermodynamics* (Springer, Berlin, 1969), Vol. 1, p. 338.
[9] R. Klement, D. M. Soumpasis, and T. Jovin, Proc. Natl. Acad. Sci. U.S.A. **88**, 4631 (1991).
[10] R. Klement, in *Computation of Biomolecular Structures*, edited by D. M. Soumpasis and T. Jovin (Springer, Berlin, 1993), p. 207.
[11] J. G. Kirkwood, J. Chem. Phys. **3**, 300 (1935).
[12] I. Z. Fisher and B. L. Kopeliovich, Dokl. Akad. Nauk SSSR **133**, 81 (1960) [Sov. Phys.—Dokl. **5**, 761 (1960)].
[13] J. G. Kirkwood and F. P. Buff, J. Chem. Phys. **17**, 338 (1949).
[14] D. Eisenberg and W. Kauzmann, *The Structure and Properties of Water* (Oxford University Press, New York, 1969), p. 78.
[15] D. M. Soumpasis, P. Procacci, and G. Corongiu, IBM DSD Report, 1991 (unpublished).
[16] U. Niesar, G. Corongiu, E. Clementi, G. R. Kneller, and D. K. Bhattacharya, J. Phys. Chem. **94**, 7949 (1990).
[17] H. J. C. Berendsen, J. P. M. Postma, W. F. van Gunsteren, and J. Hermans, in *Intermolecular Forces*, edited by B. Pullmann (Reidel, Dordrecht, 1981), p. 331.
[18] D. L. Beveridge, M. Mezei, P. K. Mehrotra, F. T. Marchese, G. Ravi-Shanker, T. Vasu, and S. Swaminathan, in *Molecular Based Study of Fluids*, Advances in Chemistry Series 204, edited by J. M. Haile and G. A. Mansoori (American Chemical Society, Washington, DC, 1983), p. 297.
[19] N. Metropolis, A. W. Rosenbluth, M. N. Rosenbluth, A. H. Teller, and E. Teller, J. Chem. Phys. **21**, 1087 (1953).
[20] H. E. Alper and R. M. Levy, J. Chem. Phys. **91**, 1242 (1989).
[21] M. Belhadj, H. E. Alper, and R. M. Levy, Chem. Phys. Lett. **179**, 13 (1991).
[22] *The Problem of Long-Range Forces in the Computer Sim-*

ulation of Condensed Media, edited by D. Ceperley, National Resource for Computation in Chemistry, Proceedings No. 9, Report No. LBL-10634 of the Lawrence Berkeley Laboratory, University of California, 1980.
[23] D. J. Adams, J. Chem. Phys. **78**, 2585 (1983).
[24] C. L. Brooks, B. M. Pettitt, and M. Karplus, J. Chem. Phys. **83**, 5897 (1985).
[25] P. Linse and H. C. Andersen, J. Chem. Phys. **85**, 3027 (1986).
[26] G. Hummer, D. M. Soumpasis, and M. Neumann, Mol. Phys. **77**, 769 (1992).
[27] G. Hummer and M. Neumann (unpublished).
[28] M. Neumann, Mol. Phys. **50**, 841 (1983).
[29] In the MC simulations of the ice-water interface described in the following, the GRF treatment of the electrostatic interactions was three times faster than Ewald summation.
[30] G. Hummer and D. M. Soumpasis, J. Chem. Phys. **98**, 581 (1993).
[31] S. W. DeLeeuw, J. W. Perram, and E. R. Smith, Proc. R. Soc. London Ser. A **373**, 27 (1980).